Electronic Structure and Bonding in $CuMO_2$ (M = Al, Ga, Y) Delafossite-Type Oxides: An Ab Initio Study

Antonio Buljan, Pere Alemany,* and Eliseo Ruiz

Centre Especial de Recerca en Química Teòrica (CERQT) and Departaments de Química Física i de Química Inorgànica, Universitat de Barcelona, Diagonal 647, 08028 Barcelona, Catalunya, Spain

Received: November 12, 1998; In Final Form: July 19, 1999

The structural and electronic properties of some simple ternary oxides with the delafossite-type structure have been investigated using the periodic Hartree−Fock method and a posteriori density-functional corrections. The coexistence in the same crystal structure of different structural motifs, such as MO_6 octahedra, linear O−Cu−O units, and hexagonal Cu layers with relatively short Cu−Cu distances, enables accurate calculation of the structural data for this type of material rather difficult: correlation effects seem only to be important for the description of the Cu−O bonds, while the geometry of the MO_6 octahedra is best described by the Hartree−Fock method. The analysis of bonding in the Cu layers reveals the existence of weak d^{10}−d^{10} interactions that are suggested to be important in the determination of the electrooptical properties of doped delafossites.

I. Introduction

A large number of ternary noble metal oxides of the AMO_2 type crystallize in the relatively simple delafossite ($CuFeO_2$) structure.[1,2] In these compounds A is usually Pt, Pd, Ag, or Cu, while almost any trivalent cation (Al, Sc, Cr, Fe, Co, Ga, Rh, In, La, Y, Pr, Nd, Sm, Eu, and Tl) can be used as M.[3−5] The large variation in chemical and physical properties of these materials is in the origin of the diverse technological applications that have been suggested for them. Delafossites are currently being employed as catalysts (synthesis of methanol using $CuCrO_2$,[6] conversion of toxic gases emanated by internal combustion engines using $CuFeO_2$,[7,8] an O_2 electrocatalysis using delafossites where A = Pt and Pd[9]) and as electrode materials in Zn−air batteries ($AgNiO_2$).[10] Recently they have also been suggested for use in solar applications, such as functional windows that transmit visible light while generating electricity in response to the absorption of ultraviolet photons ($CuAlO_2$).[11]

Despite the interest that these materials have received from an experimental point of view, the electronic structure and bonding in this family of oxides remains relatively unknown. Interpretation of experimental data on structural and electrical properties of delafossites up to the present has been based on the qualitative band structure model proposed by Rogers et al.[12] in 1971. The first accurate calculation of the electronic structure for a compound with the delafossite structure appeared in a work by Mattheiss[13] devoted to the problem of oxygen doping in $CuYO_2$. Recently, Seshadri et al.[14] have used LMTO-ASA electronic structure calculations to analyze the influence of metal−metal bonding in the metallic behavior of some delafossites.

In the present work we try to deepen the understanding of the electronic structure of delafossites by analyzing the electronic structure in three semiconducting delafossites ($CuMO_2$ with M = Al, Ga, and Y) by means of periodic ab initio calculations of the Hartree−Fock type. The calculations presented in this paper were largely motivated by the aim of analyzing the nature of bonding in the delafossites, especially with regard to the hexagonal copper layers. Weak closed shell d^{10}−d^{10} interactions have been found to play an important role in the structural and physical properties of organometallic compounds[15] but remain mostly unexplored in solid state, extended structures. Since this type of interactions has been recently proposed to play an important role in their electrooptical properties,[11] we think that bonding in the copper layers of semiconducting delafossites deserves a more thorough investigation. During our study we have found that the delafossite-type structure, with three different structural motifs in the same crystal (MO_6 octahedra, linear O−Cu−O units, and hexagonal Cu layers), offers a very stringent test for the applicability of modern electronic structure methods to the structural optimization of complex solids.

II. Methodology

Calculations reported in this work have been performed using the CRYSTAL-95 program, which provides self-consistent solutions to the Hartree−Fock-Roothan equations subject to periodic boundary conditions.[16,17] Electronic correlation has been considered in the present work by including a posteriori density functional corrections to the Hartree−Fock (HF) total energy[18−21] using either the correlation functional proposed by Lee, Yang, and Parr (LYP)[22] or that proposed by Perdew and Wang (PW).[23,24] Details on the mathematical formulation of the computational methods employed in this work have been previously described in the literature and will be omitted here.[17]

In the CRYSTAL-95[16,17] program, Bloch functions are constructed as linear combinations of an orbital basis set derived from atomic centered Gaussian-type functions. As in molecular HF calculations, the results can be quite sensitive to the choice of this basis set. A more detailed description of the basis sets adopted in this work for each element can be found in the

* To whom correspondence should be addressed. Departament de Química Física, Universitat de Barcelona. Diagonal 647, 08028 Barcelona, Catalunya, Spain. E-mail: pere@linus.qui.ub.es.

10.1021/jp984420a CCC: $18.00
Published on Web 09/08/1999

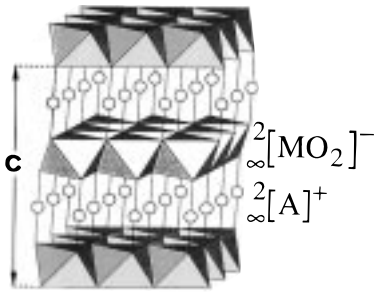

Figure 1. Stacking of $[^2_\infty MO_2]^-$ and $[^2_\infty A]^+$ layers in the crystal structure of hexagonal (2H) AMO_2 delafossites.

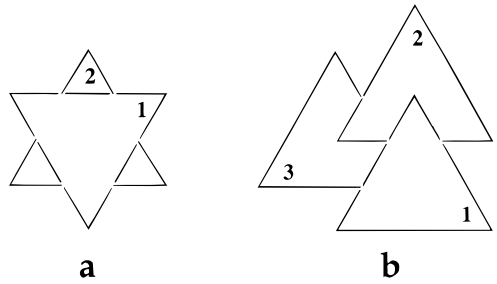

Figure 2. Schematic representation of the arrangement of $[^2_\infty MO_2]^-$ layers in the 2H polytype (a) and in the 3R polytype (b) of AMO_2 delafossites. For each MO_6 octahedron only the upper triangular face is represented. Numbers in each triangle indicate the succesive $[^2_\infty MO_2]^-$ layers.

Appendix. Computational parameters controlling the truncation of both the Coulomb and exchange infinite series have been chosen following the recommendations given by Pisani et al.[17] in order to obtain a good level of accuracy for the calculated energies.

III. Results

Crystal Structure. Delafossite-type AMO_2 oxides crystallize in a simple structure (Figure 1) built of infinite one-octahedron-thick sheets of close-packed MO_6 octahedra. These layers are linked together by the A atoms, forming linear O−A−O units which are appropriate for A^+ cations. The stacking of successive layers of MO_6 octahedra can result in different polytypes. The difference between the structures of the two most common polytypes, known as 3R and 2H delafossites, is shown schematically in Figure 2. In the trigonal 3R (*R*-3*m*, no. 166) crystal structure there are three layers per unit cell and the fourth layer coincides with the first one. Using hexagonal axes for the unit cell one finds an average value of 18 Å for the *c*-parameter, while the *a*-parameter is strongly dependent on the nature of the M^{3+} cation. The atomic positions in this structure[25] are all fixed by symmetry except the z-value of the oxygen atoms. The hexagonal ($P6_3/mmc$, no. 194) 2H-delafossites contain only two layers per unit cell, with an average *c*-parameter of 12 Å. As in the case of the 3R polymorph, the atomic positions in this structure[26] are all fixed by symmetry except the *z*-value of the oxygen atoms.

Results of the geometrical optimization of the crystal structure for some selected delafossite-type oxides are presented in Table 1. Comparison with other computational studies is not possible because, to the best of our knowledge, no geometry optimizations have been reported in the literature for this family of compounds.

TABLE 1: Calculated Lattice Parameters, Interatomic Distances, and Bulk Moduli for Some Delafossite-Type Oxides Using the Hartree−Fock Method (HF) and Hartree−Fock plus a posteriori Correlation Energy Corrections Using the Lee−Yang−Parr (HF+LYP) or the Perdew-Wang (HF+PW) Functionals, and Available Experimental Data Reported for Comparison

2H−$CuAlO_2$	*a* (Å)	*c* (Å)	*z*	Cu−O (Å)	M−O (Å)	*B* (GPa)
HF	2.856	11.466	0.0835	1.909	1.907	211
HF+PW	2.799	11.263	0.0839	1.871	1.872	
HF+LYP	2.777	11.206	0.0843	1.857	1.861	
exptl	2.863	11.314	0.0851	1.866	1.913	
3R−$CuAlO_2$						
HF	2.857	17.197	0.1110	1.909	1.907	204
HF+PW	2.774	16.794	0.1104	1.854	1.860	
HF+LYP	2.797	16.892	0.1108	1.871	1.871	
exptl	2.858	16.958	0.1099	1.864	1.910	
2H−$CuGaO_2$						
HF	2.973	11.595	0.0853	1.910	1.981	192
HF+PW	2.913	11.455	0.0873	1.864	1.957	
HF+LYP	2.931	11.340	0.0862	1.867	1.957	
3R−$CuGaO_2$						
HF	2.970	17.388	0.1098	1.909	1.979	192
HF+PW	2.888	17.018	0.1111	1.891	1.917	
HF+LYP	2.928	17.108	0.1091	1.866	1.956	
exptl	2.977	17.171	0.1076	1.848	1.996	
2H−$CuYO_2$						
HF	3.540	11.620	0.0894	1.866	2.293	126
HF+PW	3.454	11.586	0.0912	1.840	2.256	
HF+LYP	3.461	11.601	0.0913	1.841	2.262	
exptl	3.531	11.418	0.0893	1.835	2.274	
3R−$CuYO_2$						
HF	3.544	17.186	0.1072	1.842	2.287	129
HF+PW	3.474	17.146	0.1072	1.838	2.250	
HF+LYP	3.487	17.220	0.1068	1.839	2.262	
exptl	3.533	17.136	0.1066	1.827	2.285	

The optimization of the crystal structure for delafossite-type oxides using ab initio electronic structure methods can be considered as a very stringent test for the performance of these methods. The coexistence in the same crystal structure of different structural units (MO_6 layers, O−Cu−O fragments, and metal-like hexagonal Cu layers) makes an accurate prediction of the structural data very difficult. Bond distances in the MO_6 layers and the value for the cell constant *a* are properly reproduced by the HF method, with average errors of 0.27% for *a* and 0.45% for M−O, respectively. These average errors are in the same range as those obtained by Dovesi et al. for other ionic compounds.[17] Inclusion of the correlation energy results in an underestimation of these two quantities with average errors of about 2% irrespective of the functional that is employed.

The cell constant *c* and the Cu−O distance are however overestimated by the HF method (average errors of 1.2% and 2.1% for *c* and Cu−O respectively). The consideration of electronic correlation, which is especially important for an accurate description of covalent bonds in solids, through density functional theory reduces both *c* and the Cu−O distance, decreasing the average error for these two quantities to less than 0.8%. Similar results have been previously reported for the related Cu_2O structure.[27] The performance of the two functionals employed in the present work is similar, although slightly better average results are obtained with the LYP functional. It would be interesting to compare these results with calculations in which correlation effects are included in a self-consistent way and not as an a posteriori correction, although such comparison is not

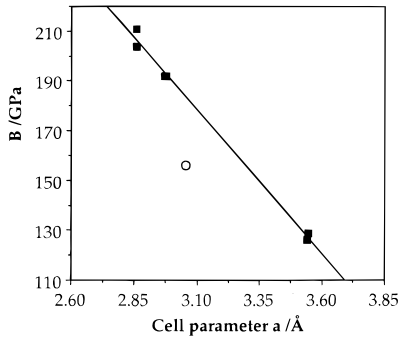

Figure 3. Variation of the calculated bulk modulus (B) as a function of the cell constant *a* for the three delafossites studied in this work (solid squares). The experimentally determined bulk modulus of 3R−$CuFeO_2$ is indicated by an empty circle.

straightforward since changes in the basis set or in the numerical approximations used in different programs can lead to significant differences. Comparison of geometry optimizations for some alkaline earth oxides using both methodologies[20,28] shows, however, that the deviation of optimized parameters from their Hartree−Fock values because of the way in which correlation is included in the calculations is of the same order of those changes obtained when using different functionals. This fact seems to indicate that our main conclusion, i.e., that correlation affects mainly the Cu−O distance in delafossites, is essentially correct despite the way in which correlation effects are considered.

These findings reflect that although they can be classified as ionic insulators, the bonding situation in delafossites is far from trivial. Cu−O bonding in the linear O−Cu−O fragments has a considerable covalent character, while M−O bonds in MO_6 octahedra are strongly ionic. On the other hand, the Cu−Cu distances of 2.86 Å in $CuAlO_2$ are only slightly longer than those found in metallic copper (2.56 Å) and some kind of Cu^+−Cu^+ attractive interaction is expected (see below).

As far as the relative stability of the 2H and the 3R phases of these compounds is concerned, our calculations indicate that the 2H phases of all three compounds should be more stable by 0.1−0.2 kcal/mol than the 3R ones. These small energy differences are however at the limits of accuracy of our computational method and should be taken only as an indication that both phases have very similar stabilities, in concordance with the experimental observations[29] which indicate that it is very difficult to predict the appearance of one of both polytypes from the conditions employed in the synthetic process.

The isotropic variation of the volume of the unit cell has been used for the determination of the bulk modulus for all six crystal structures. A plot of the calculated bulk modulus as a function of the cell parameter *a* (Figure 3) shows a linear relation between these two quantities: the larger the cell constant, the smaller the bulk modulus of the compound. Although there are no available experimental data for these three compounds, the experimentally determined value for the bulk modulus of $CuFeO_2$ (156 GPa) agrees qualitatively with this trend.[30,31] No correlation is found between *c* and the bulk modulus, indicating that this property is basically determined by the strong ionic interactions in the MO_6 layers, and is practically independent of the geometry of the O−Cu−O units and should therefore be correctly described at the HF level of theory.

An interesting structural feature of the delafossite-type compounds is the departure of the coordination environment of the trivalent M^{3+} ions from its ideal octahedral symmetry. In all delafossites, these octahedra are slightly flattened in the direction of the crystal *c* axis and their degree of distortion can be measured by the ratio of the O−O distance found in the hexagonal O layers (d_0) and that between two consecutive layers (d_1) (Figure 4a, inset). The correlation found between this ratio and the ionic radius of the M^{3+} cation (Figure 4a) is on the basis of the suggestion that the distortion of the octahedra is mainly due to the electrostatic repulsion of neighboring M^{3+} ions.[32,33] To verify this hypothesis we have investigated the variation of the total energy with the degree of distortion of the MO_6 octahedra for the 2H polymorph of $CuAlO_2$ in two different ways: by using the HF method and by considering only the electrostatic interaction of the charged ions (Cu^+, Al^{3+}, and O^{2-}).[34,35] In both cases (Figure 4b) the distorted structure is preferred over the ideal one, indicating that, as previously suggested, the purely electrostatic repulsion between neighboring M^{3+} ions is playing the leading role in the observed trend.

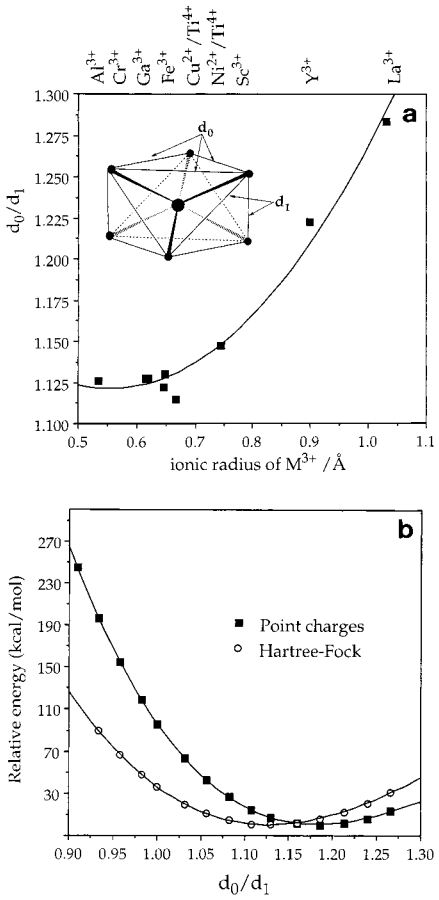

Figure 4. (a) Deformation of MO_6 octahedra as a function of the ionic radius of the M^{3+} cations. (b) Variation of the Hartree−Fock and the purely electrostatic energies as a function of d_0/d_1 for a model based on the 2H−$CuAlO_2$ phase.

Band Structure and Density of States. The calculated band structures of 2H- and 3R-$CuAlO_2$ are presented in Figure 5. The results show the existence of large indirect band gaps for both phases, in good agreement with the insulating behavior found for these oxides.[36−38] The calculated band gaps of 11.65 eV (2H polytype) and 11.78 eV (3R polytype) are nevertheless strongly overestimated in these calculations when compared to the photoelectrochemical measurements of Benko et al. that suggest an indirect gap of approximately 1.65 eV for 3R−$CuAlO_2$.[36] This large discrepancy reflects the well-known inability of the Hartree−Fock method in the calculation of this property.[17]

The calculated total density of states (DOS) and its orbital-projected contributions for the 2H polytype of $CuAlO_2$ are

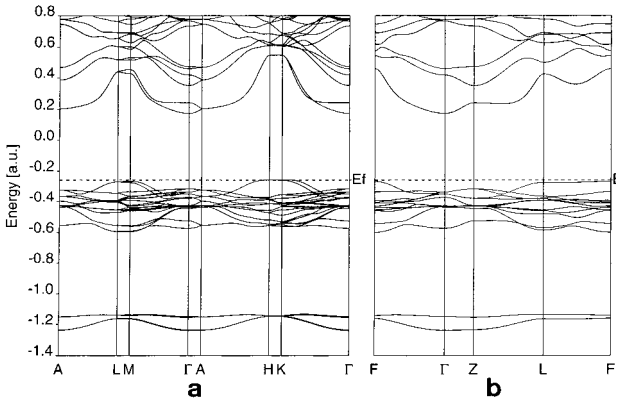

Figure 5. Electronic band structure for $CuAlO_2$. (a) 2H polytype, (b) 3R polytype.

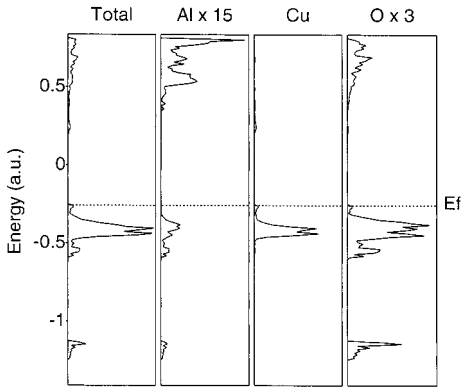

Figure 6. Atomic orbital projections of the density of states (DOS) obtained for 2H−$CuAlO_2$. The atomic orbital contributions have been evaluated using a Mulliken partition scheme.

displayed in Figure 6. The valence band is dominated by the Cu 3d states, while the contribution of the 4p states is practically zero. The 4s Cu states show a small contribution to the valence band, in good agreement with the Orgel model that proposes an s−d_{z^2} hybridization (with the Cu−O bonds on the *z*-axis) for linearly coordinated Cu^+ ions.[39] Following this qualitative model, the lower part of the conduction band is dominated by Cu 4s states with some admixture of the Cu $3d_{z^2}$ orbital. Aluminum states have a negligible contribution to the valence band and to the lower part of the conduction band, with important contributions only at relatively high energies in the upper zone of the conduction band. The only contribution from the O atoms to the valence band comes from the 2p states which appear overlapped with the sharp Cu 3d peak. Oxygen 2s states appear in a separated band approximately 0.5 au below the valence band. A very similar DOS diagram has been calculated for the 3R polytype of $CuAlO_2$, indicating that, as expected, bonding is qualitatively identical in both phases.

Figures 7a and b show the DOS and their atom-projected contributions for the 2H polytypes of $CuGaO_2$ and $CuYO_2$. The copper and oxygen contributions to the total DOS in these compounds are very similar to those found in $CuAlO_2$. The top of the valence band is formed by s−d_{z^2} hybrid orbitals in good agreement with the qualitative model proposed by Orgel.[39] Significant differences appear for $CuGaO_2$ in the low energy region, where a sharp peak, associated with strongly localized 3d states of Ga appears. In the case of $CuYO_2$, the most relevant features are the relatively narrow valence band, the Y-4p contribution in the region below the valence band, and the important contribution of Y-4d states in the lower edge of the

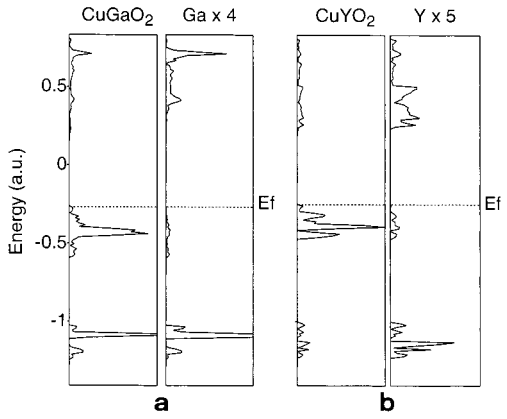

Figure 7. Atomic orbital projections of the density of states (DOS) obtained for hexagonal (a) $CuGaO_2$ and (b) $CuYO_2$.

conduction band. The large Cu−Cu distances (3.54 Å) that imply a small overlap between neighboring atoms are responsible of the narrow valence band in this compound. From all three delafossites studied in this work, $CuYO_2$ is the only one in which the orbitals of the M^{3+} ions have a significant participation in the states around the band gap. This finding is in disagreement with the interpretation of experimental data given by Benko and Koffyberg[40] who suggested that the trivalent ions in the delafossite type oxides are electronically inactive and influence the band structure only indirectly via the size of the unit cell. While this suggestion is valid for $CuAlO_2$ and $CuGaO_2$, it clearly does not apply to $CuYO_2$ where the width of the band gap is influenced by the 4d states of Y that appear at the lower edge of the conduction band.

Electron Density and Bonding in the Metal Layers. Electron density maps were calculated for the 2H polytypes of all three delafossites. Figure 8a−f display the total electron density and the difference between the electron density in the crystal and that obtained from the superposition of the spherical atomic densities for three different planes in the 2H−$CuAlO_2$ crystal. The electron density map for the copper layer (Figure 8a) shows a practically spherical distribution of the electron density around the copper atoms. The difference map in Figure 8b shows clearly that formation of these layers results in an accumulation of charge density both between each copper pair and in the center of each Cu triangle. Although the details of these electron density maps differ from those obtained experimentally by Ishiguro et al.,[41] both the calculated and the experimental maps indicate the accumulation of charge density in the center of the copper triangles.

In the electron density map for the plane containing the Cu−O bonds (Figure 8c), the electron density around copper and oxygen atoms presents a noticeable deformation in the direction of the Cu−O bonds, indicating a nonnegligible covalent character for these bonds. The difference map (Figure 8d) shows that copper atoms are donating electron density to the oxygen atoms, mainly from the $3d_{z^2}$ orbitals, a situation that is very similar to that found in an earlier paper for Cu_2O.[27]

Figure 8e shows the electron density map for a plane containing Al−O bonds. An almost perfectly spherical charge distribution around Al atoms is indicative of the strongly ionic nature of the interactions in the AlO_2 layers. The difference map in Figure 8f indicates that in these layers, as expected, charge is being transferred from aluminum to oxygen.

The electron density maps for $CuGaO_2$ and $CuYO_2$ are qualitatively very similar to those in $CuAlO_2$ and will not be discussed in detail. An interesting question is however the degree

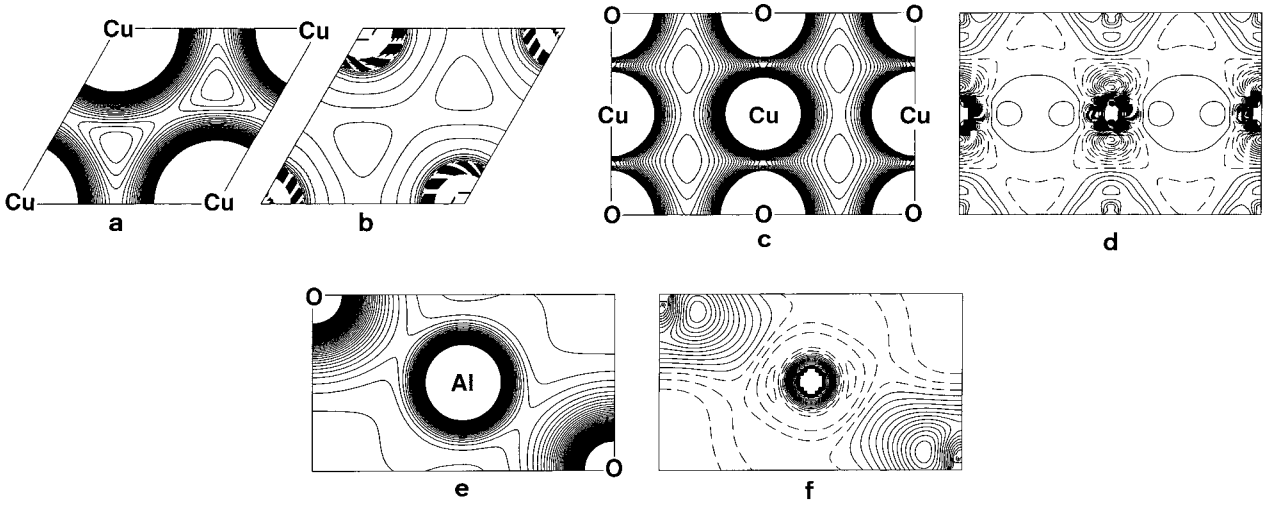

Figure 8. Electronic charge density maps calculated for selected planes of 2H−$CuAlO_2$. Total electron density (a, c, and e) and electronic density difference between the crystal and the corresponding spherical atomic density superposition arrays (b, d, and f) are represented for the [001] plane (a, b), the [100] plane (c, d) and the [1$\bar{2}$0] plane (e, f). Values corresponding to neighboring isodensity lines differ by 0.002 e^-/bohr^3 in (a, b, e, and f) and 0.005 e^-/bohr^3 in (c and d).

TABLE 2: Mulliken Net Charges (in Electrons) for the 2H Polytypes of the $CuMO_2$ Oxides Studied in This Work

compound	q(Cu)	q(M)	q(O)
$CuAlO_2$	+0.78	+2.38	−1.58
$CuGaO_2$	+0.78	+2.06	−1.42
$CuYO_2$	+0.76	+2.29	−1.52

of ionicity in the MO_2 layers in all three compounds. The results of a Mulliken population analysis (Table 2) indicate that $CuAlO_2$ presents the most ionic MO_2 layers of all three compounds, while those in $CuGaO_2$ are the less ionic ones. The charge on the copper atoms is very similar for all three compounds and in the same range as that calculated for Cu_2O in an earlier work[27] using the same method, indicating a bonding situation close to a fully ionic picture, with Cu^+ ions in the structure. The population analysis for the 3R polytypes yields practically the same charges as for the 2H polytypes, showing that the atomic charges in these compounds are mainly dictated by the local environment of each atom and independent of the long-range structure of the crystal.

An interesting question which is worthwhile to explore is the existence of attractive interactions between the Cu atoms present in these compounds. Closed shell $d^{10}-d^{10}$ interactions have been found to be important in determining the structure and physical properties of several molecules and crystals that exhibit relatively short $Cu^+\cdots Cu^+$ distances.[15,42] Recent calculations show that this type of interactions are responsible for an important part of the interaction energy between the two interpenetrated sublattices of Cu_2O, amounting roughly −1.0 kcal/mol per each Cu···Cu contact.[27]

The presence of $d^{10}-d^{10}$ attractive interactions in the delafossite-type compounds studied in this work has been detected by means of a topological analysis of the electron density in the copper layers of the 2H polytypes of all three compounds.[43−49] This analysis reveals the existence of these interactions which show up as a bond critical point in the electron density between each copper pair and a ring critical point in the center of each copper triangle. The electron density found at each of these critical points is indicated in Table 3.

The electron density at the critical points decreases almost linearly with the Cu···Cu distance. These results are in agreement with those found by Alvarez et al.[50] for [Cu(NH_3)Cl] dimers, showing that $d^{10}-d^{10}$ interactions of the same type exist both in molecular and extended structures. A detailed study of the influence of these $d^{10}-d^{10}$ interactions on the electrooptical properties of delafossite-type oxides and in related compounds will be published in short time.

TABLE 3: Electron Density at the Bond and Ring Critical Points in the Cu Layers of the 2H Polytypes of the Three Delafossite Compounds Studied in This Work, and Data for Cuprite Provided for Comparison

compound	ρ (bond)	ρ (ring)	Cu···Cu (Å)
$CuAlO_2$	0.013	0.006	2.856
$CuGaO_2$	0.010	0.005	2.973
$CuYO_2$	0.003	0.001	3.540
Cu_2O	0.007	0.003	3.004

IV. Conclusions

The Hartree−Fock method and a posteriori density-functional corrections have been used in the investigation of the structural and electronic properties of some simple ternary oxides with the delafossite-type structure. The coexistence in the same crystal structure of different structural units (MO_6 layers, O−Cu−O fragments, and metal-like hexagonal Cu layers) makes an accurate calculation of the structural data for these compounds rather difficult: correlation effects seem only to be important for an accurate description of the Cu−O bonds, while the geometry of the MO_6 octahedra is best described by the Hartree−Fock method. The bulk modulus and the deformation of the MO_6 octahedra are found to be mainly determined by ionic interactions between the M^{3+} cations and the oxygen anions and are consequently well described at the Hartree−Fock level.

An analysis by means of the density of states and its orbital-projected contributions reveals that, in good agreement with the Orgel model for linearly coordinated Cu^+ ions,[39] the valence band is dominated by the Cu 3d states, while the contribution of the 4p states is practically zero. The 4s Cu states show a small contribution to the valence band, in good agreement with the s−d_{z^2} hybridization proposed in this qualitative model. The lower part of the conduction band is dominated by Cu 4s states with some admixture of the Cu 3d_{z^2} orbital, except for the case when M = Y where 4d states of Y appear at the lower edge of the conduction band. Weak $d^{10}-d^{10}$ interactions in the hexagonal

TABLE 4. Exponents ($bohr^{-2}$) and Contraction Coefficients (coeff) of the Gaussian Functions Adopted in This Work

O			Cu		Al			Y		Ga		
	exp	s coeff	p,d coeff	exp	coeff		exp	s coeff	p,d coeff	exp	coeff		exp	s coeff	p,d coeff
s	8020.000	0.0011		s 76441.484	0.0142	s	59852.600	0.0004		s 147197.000	0.0016	s	444668.000	0.0002	
	1338.000	0.0080		11477.790	0.0109		8507.900	0.0034		22066.570	0.0125		64576.800	0.0019	
	255.400	0.0532		2611.477	0.0541		1902.550	0.0173		5005.389	0.0630		13935.200	0.0108	
	69.220	0.1681		737.335	0.1886		562.450	0.0617		1406.386	0.2191		3651.660	0.0490	
	23.900	0.3581		240.028	0.3834		202.931	0.1680		455.537	0.4655		1099.410	0.1672	
	9.264	0.3855		82.721	0.2965		77.677	0.3850		156.283	0.3793		381.106	0.3643	
	3.851	0.1468		s 160.074	−0.1104		31.150	0.5224		s 298.951	0.1108		149.482	0.4028	
	1.212	0.0728		18.854	0.6459		12.431	0.2864		35.782	−0.6294		62.817	0.1477	
sp	49.430	−0.0088	0.0096	7.744	0.4451	sp	565.087	−0.0004	0.0011	15.071	−0.4450	sp	1155.650	−0.0060	0.0088
	10.470	−0.0915	0.0696	s 13.679	−0.2269		144.448	−0.0059	0.0075	s 27.842	0.2423		278.060	−0.0700	0.0630
	3.235	−0.0402	0.2065	2.258	0.7240		50.146	−0.0385	0.0339	4.732	−0.7531		93.190	−0.1400	0.2196
	1.217	0.3790	0.3470	s 0.925	1.0000		18.998	−0.0964	0.1160	2.084	−0.3833		37.095	0.2685	0.4083
sp	0.450	1.0000	1.0000	s 0.410	1.0000		8.036	0.0204	0.2451	s 3.629	0.2725		15.482	0.6184	0.4154
sp	0.200	1.0000	1.0000	s 0.150	1.0000		3.588	0.3772	0.3701	0.996	−0.7660		5.152	0.3248	0.3536
d	0.750	1.0000	1.0000	p 2530.017	0.0019		1.588	0.5164	0.3554	s 1.143	1.0000	sp	70.621	0.0067	−0.0085
				600.092	0.0158		0.708	0.1783	0.1356	s 0.580	1.0000		27.178	−0.0863	−0.0350
				194.094	0.0763	sp	1.960	−0.0607	0.0514	s 0.310	1.0000		11.439	−0.346	0.0849
				p 73.686	0.2388		0.855	−0.1183	−0.0938	p 2045.561	−0.0078		4.624	0.4086	0.5583
				30.459	0.4498	sp	0.560	1.0000	1.0000	483.065	−0.0602	sp	1.829	1.0000	1.0000
				13.131	0.3936	sp	0.350	1.0000	1.0000	153.453	−0.2425	sp	0.663	1.0000	1.0000
				p 5.526	1.0000	d	0.580		1.0000	55.792	−0.5036	sp	0.198	1.0000	1.0000
				p 2.149	1.0000					20.935	−0.3600	d	67.427		0.0259
				p 0.769	1.0000					p 11.448	−0.3352		18.837		0.1495
				d 51.443	0.0293					4.760	−0.5433		6.306		0.3805
				14.404	0.1570					p 2.040	1.0000		2.130		0.4768
				4.848	0.3779					p 1.182	1.0000	d	0.676		1.0000
				d 0.619	1.0000					p 0.200	1.0000				
				d 0.476	1.0000					d 163.473	0.0175				
										47.645	0.1139				
										17.066	0.3404				
										6.399	0.2938				
										d 1.523	0.0888				
										0.563	0.3771				
										d 0.140	1.0000				

Cu layers, which are important in the determination of the physical and structural properties of these compounds, have been detected in a topological analysis of the electron density.

Acknowledgment. The authors are grateful to S. Alvarez and E. Canadell for helpful comments on this work and to C. Gatti for providing them with a copy of the TOPOND-96 program. A.B. thanks the *Agencia Española de Cooperación Internacional* for a MUTIS fellowship. Financial support to this work was provided by DGYCIT (project PB95-0848-CO2-01) and CIRIT (grant 1995SGR-00421). The computing resources at the *Centre de Supercomputació de Catalunya* (CESCA) were partly made available through a grant from the University of Barcelona and the *Fundació Catalana per a la Recerca*.

Appendix

In the calculations presented in this work every atomic orbital is expressed as the product of an angular real solid harmonic function by a linear combination of radial Gaussian-type functions. These functions have been adapted from different molecular basis sets (ref 51 for O, ref 52 for Cu, refs 53 and 54 for Al, ref 55 for Ga, and ref 56 for Y). The contraction patterns employed for each atom are: (8411/411/1) for O, (632111/33111/311) for Cu, (88211/8211/1) for Al, (864111/64111/41) for Ga, and (6332111/521111/521) for Y. A detailed description of exponents and contraction coefficients of the Gaussian functions is given in Table 4.

References and Notes

(1) Soller, W.; Thompson, A. J. *Phys. Rev.* **1935**, *47*, 644.
(2) Soller, W.; Thompson, A. J. *Bull. Am. Phys. Soc.* **1935**, *10*, 17.
(3) Hahn, H.; Lorent, C. *Z. Anorg. Allg. Chem.* **1955**, *279*, 281.
(4) Haas, H.; Kordes, E. *Z. Kristallogr.* **1969**, *129*, 259.
(5) Prewitt, C. T.; Shannon, R. D.; Rogers, D. B. *Inorg. Chem.* **1971**, *10*, 719.
(6) Monnier, J. R.; Hanrahan, M. J.; Apai, G. *J. Catal.* **1985**, *92*, 119.
(7) Carreiro, L. *Mater. Res. Bull.* **1985**, *20*, 619.
(8) Christopher, J.; Swamy, C. S. *J. Mater. Sci.* **1992**, *27*, 1353.
(9) Carcia, P. F.; Shannon, R. D.; Biertedt, P. E.; Flippen, R. B. *J. Electrochem. Soc.* **1980**, *127*, 1974.
(10) RAY O. Vac Co. *Jpn Kokai Tokkyo Koho 8276*, pp 745, 756, 757.
(11) Kawazoe, H.; Yasukawa, M.; Hyodo, H.; Kurita, M.; Yanagi, H.; Hosono, H. *Nature* **1997**, *389*, 939.
(12) Rogers, D. B.; Shannon, R. D.; Prewitt, C. T.; Gillson, J. L. *Inorg. Chem.* **1971**, *10*, 723.
(13) Mattheiss, L. F. *Phys. Rev. B* **1993**, *48*, 18300.
(14) Seshadri, R.; Felser, C.; Thieme, K.; Tremel, W. *Chem. Mater.* **1998**, *10*, 2189.
(15) Pyykkö, P. *Chem. Rev.* **1997**, *97*, 597.
(16) Dovesi, R.; Saunders: V. R.; Roetti, C.; Causà, M.; Harrison, N. M.; Orlando, R.; Aprà, E. *CRYSTAL95*; University of Torino: Italy, Daresbury Laboratory: U.K., 1996.
(17) Pisani, C., Ed. *Quantum-Mechanical Ab initio Calculation of the Properties of Crystalline Materials*; Springer-Verlag: Berlin, 1996.
(18) Causà, M.; Dovesi, R.; Pisani, C.; Colle, R.; Fortunelli, A. *Phys. Rev. B* **1987**, *36*, 891.
(19) Causà, M.; Colle, R.; Fortunelli, A.; Dovesi, R. *Phys. Scr.* **1988**, *194*, 38.
(20) Causà, M.; Zupan, A. *Chem. Phys. Lett.* **1994**, *220*, 145.
(21) Lichanot, A.; Merawa, M.; Causà, M. *Chem. Phys. Lett.* **1995**, *246*, 263.
(22) Lee, C.; Yang, W.; Parr, R. G. *Phys. Rev. B* **1988**, *37*, 785.
(23) Perdew, J. P.; Wang, Y. *Phys. Rev. B* **1986**, *33*, 8800.
(24) Perdew, J. P.; Wang, Y. *Phys. Rev. B* **1992**, *45*, 13244.
(25) The atomic fractional coordinates for the 3R polytype of the AMO_2 delafossite structure are *A* (3a) 0, 0, 0; *M* (3b) 0, 0, 1/2; *O* (6c) 0, 0, *z*.
(26) The atomic fractional coordinates for the 2H polytype of the AMO_2 delafossite structure are *A* (2c) 1/3, 2/3, 1/4; *M* (2a) 0, 0, 0; O (4f) 1/3, 2/3, *z*.
(27) Ruiz, E.; Alvarez, S.; Alemany, P.; Evarestov, R. A. *Phys. Rev. B* **1997**, *56*, 7189.

(28) Habas, M. P.; Dovesi, R.; Lichanot, A. *J. Phys.*: *Condens. Matter* **1998**, *10*, 6897.
(29) Isawa, K.; Yaegashi, Y.; Komatsu, M.; Nagano, N.; Sudo, S.; Karppinen, M.; Yamauchi, H. *Phys. Rev. B* **1997**, *56*, 3457.
(30) Zhao, T. R.; Hasegawa, M.; Takei, H.; Kondo, T.; Yagi, T. *Jpn. J. Appl. Phys.* **1996**, *35*, 3535.
(31) Zhao, T. R.; Hasegawa, M.; Kondo, T.; Yagi, T.; Takei, H. *Mater. Res. Bull.* **1997**, *32*, 151.
(32) Doumerc, J. P.; Wichainchai, A.; Pouchard, M.; Hagenmüller, P.; Ammar, A. *J. Phys. Chem. Solids* **1987**, *48*, 37.
(33) Ishiguro, T.; Kitazawa, A.; Mizutani, N.; Kato, M. *J. Solid State Chem.* **1983**, *40*, 564.
(34) Hoppe, R. *Angew. Chem., Int. Ed. Engl.* **1966**, *5*, 95.
(35) Hoppe, R. *Angew. Chem., Int. Ed. Engl.* **1970**, *9*, 25.
(36) Benko, F. A.; Koffyberg, F. P. *J. Phys. Chem. Solids* **1984**, *45*, 57.
(37) Benko, F. A.; Koffyberg, F. P. *Can. J. Phys.* **1985**, *63*, 1306.
(38) Benko, F. A.; Koffyberg, F. P. *Phys. Stat. Solidi A* **1986**, *94*, 231.
(39) Orgel, L. E. *J. Chem. Soc.* **1958**, 4186.
(40) Benko, F. A.; Koffyberg, F. P. *J. Phys. Chem. Solids* **1987**, *48*, 431.
(41) Ishiguro, T.; Ishizawa, N.; Mizutani, N.; Kato, M.; Tanaka, K.; Marumo, F. *Acta Crystallogr. B* **1983**, *39*, 564.
(42) Jansen, M. *Angew. Chem., Int. Ed. Engl.* **1987**, *26*, 1098.
(43) Bader, R. F. W. *Acc. Chem. Res.* **1985**, *18*, 9.
(44) Bader, R. F. W. *Chem. Rev.* **1991**, *91*, 893.
(45) Bader, R. F. W. *Atoms in Molecules. A Quantum Theory*; Clarendon Press: Oxford, 1990.
(46) Gatti, C.; Saunders: V. R.; Roetti, C. *J. Chem Phys.* **1994**, *101*, 10686.
(47) Gatti, C.; Silvi, B.; Colonna, F. *Chem. Phys. Lett.* **1995**, *247*, 135.
(48) Bianchi, R.; Gatti, C.; Adovasio, V.; Nardelli, N. *Acta Crystallogr. B* **1996**, *52*, 471.
(49) Gatti, C. *TOPOND-96*: *An Electron Density Topological Program for Systems Periodic in N* (*N* = *0*−*3*); CNR−CSRSRC: Milano, Italy, 1996.
(50) Liu, X. Y.; Mota, F.; Alemany, P.; Novoa, J. J.; Alvarez, S. *J. Chem. Soc., Chem. Comm.* **1998**, 1149.
(51) Towler, M. D.; Harrison, N. M.; McCarthy, M. I. *Phys. Rev. B* **1995**, *52*, 5375.
(52) Schaeler, A.; Horn, H.; Ahlrichs, R. *J. Chem. Phys.* **1992**, *97*, 2571.
(53) Harrison, N. M. Unpublished Results. Available in the WWW (http://gserv1.dl.ac.uk/TCS/Software/CRYSTAL).
(54) Catti, M.; Valerio, G.; Dovesi, R. *Phys. Rev B* **1994**, *49*, 14179.
(55) Pandey, R.; Jaffe, J. E.; Harrison, N. M. *J. Phys. Chem. Solids* **1994**, *55*, 1357.
(56) Godbout, N.; Salahub, D. R.; Andzelm, J.; Wimmer, E. *Can. J. Chem.* **1992**, *70*, 560.